THE INFLUENCE OF ELECTROCHEMICAL SYNTHESIS TIME ON THE PHOTOCATALYTIC PERFORMANCE OF Ag-TiO_2 COMPOSITE UNDER UV IRRADIATION

Ionela-Cristina PETCU [1], Ana T.S.C. BRANDÃO [2], Cosmin ROMANITAN [3], Oana BRINCOVEANU [4], Adina BOLDEIU [5], Iuliana MIHALACHE [6], Lucia Monica VECA [7], Carlos M. PEREIRA [8], Liana ANICAI [9], Cristina BUSUIOC [10, *], Sabrina STATE [11, *]

This research demonstrates that the time of the green electrochemical synthesis influences the photodegradation efficiency of Ag-TiO_2. While a 3h duration was previously identified as optimal, this work evaluates the composite synthesized for 5h (Ag-TiO_2-5h). According to XRD and SEM analysis, the composite exhibited a specific surface area of 19.03 m^2/g and an average crystallite size of ~22 nm. Zeta potential measurements of the TiO_2 revealed a significant surface charge of +33.83 mV at pH 3, ensuring high colloidal stability and a strong electrostatic affinity for the anionic methyl orange (MO) dye. Consequently, Ag-TiO_2-5h achieved a higher colour removal efficiency of 74.18% compared to TiO_2 (66.78%) after 360 minutes exposure to UV light, which confirms that a 3-5h interval is suitable for synthesis.

Keywords: green solvents, electrochemical synthesis time, toxic dyes, methyl orange, photodegradation, water treatment

1. Introduction

Textile industry generates a lot of pollution every year due to the toxic dyes they use. One of the most used dyes is methyl orange (MO), whose chemical

[1] PhD Student, Faculty of Chemical Engineering and Biotechnologies, National University of Science and Technology POLITEHNICA Bucharest, Romania, e-mail: ionela.petcu@gmail.com
[2] Researcher, CIQUP-Faculty of Sciences, University of Porto, Portugal, e-mail: ana.brandao@fc.up.pt
[3] Researcher, National Institute for Research and Development in Microtehnologies, IMT-Bucharest, Ilfov, Romania, e-mail: romanitan.cosmin@gmail.com
[4] Researcher, National Institute for Research and Development in Microtehnologies, IMT-Bucharest, Ilfov, Romania, e-mail: oanabrincoveanu24@gmail.com
[5] Researcher, National Institute for Research and Development in Microtehnologies, IMT-Bucharest, Ilfov, Romania, e-mail: adina.boldeiu@imt.ro
[6] Researcher, National Institute for Research and Development in Microtehnologies, IMT-Bucharest, Ilfov, Romania, e-mail: juliana.mihalache@gmail.com
[7] Researcher, National Institute for Research and Development in Microtehnologies, IMT-Bucharest, Ilfov, Romania, e-mail: monica.veca@imt.ro
[8] Researcher, CIQUP-Faculty of Sciences, University of Porto, Portugal, e-mail: cmpereir@fc.up.pt
[9] Researcher, Center of Surface Science and Nanotechnology, National University of Science and Technology POLITEHNICA Bucharest, Romania, e-mail: liana.anicai@cssnt-upb.ro
[10*] Professor, Faculty of Chemical Engineering and Biotechnologies, National University of Science and Technology POLITEHNICA Bucharest, Romania, e-mail: cristina.busuioc@upb.ro

structure is depicted in Fig. 1, an anionic azo dye which is also used in the paper, plastic and food industry [1]. MO is hard to biodegrade because it contains a strong and stable functional group (−N=N− group), which is responsible for the toxicity of the dye [2]. MO also presents high solubility in water due to the anionic sulphonic group ($–SO_3H$) in its structure, which makes it even more harmful [3]. Unfortunately, untreated waste which contains MO is discharged in the waters and contaminates the aquatic life [4]. This toxic dye can also cause a lot of serious health problems, such as nausea, dizziness and eye irritation in humans [5].

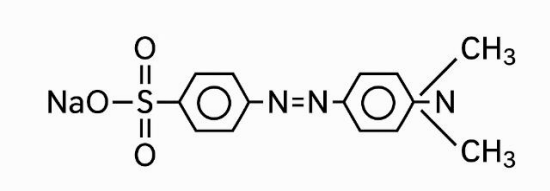

Fig. 1. 2D chemical structure of MO.

Various methods have been used to remove this dye and other dyes from wastewater. One of the most efficient and eco-friendly procedures is the photodegradation. During the photodegradation process, reactive oxidizing species (ROS) react with the dyes and lead to their decomposition [6]. Semiconductors such as zinc oxide, tin oxide or titanium dioxide are mostly used photocatalysts due to their ability to produce ROS under light irradiation [7]. Among these, titanium dioxide (TiO_2) is a versatile compound often utilized for its photocatalytic properties, particularly in applications such as environmental remediation, including the degradation of azo dyes [8, 9]. TiO_2 is biocompatible and presents a high specific surface area in powder form. In addition, it possesses remarkable electrical, mechanical and optical properties, and moreover, it can be reused. Nevertheless, TiO_2 has an intrinsic bandgap of approximately 3.23 eV, which restricts its photocatalytic capabilities to the ultraviolet (UV) region, constituting only 4 % of the solar spectrum. To overcome these limitations, several approaches have been proposed, such as doping with metal ions, coupling with semiconductors, modifying with graphene and sensitizing with dyes [10]. Recent studies also demonstrate that the photodegradation efficiency of TiO_2 can be enhanced by improving nanoparticle dispersion on various supports, such as silica fume particles, which increases the active surface area available for pollutant adsorption [11] or through the synergy between TiO_2 and inorganic cation species, facilitating also the selective degradation of complex molecules like antibiotics [12].

One of the most used methods is represented by doping/decorating TiO_2 nanoparticles (NPs) with silver (Ag) [11, 12]. Compared to TiO_2 NPs, it was demonstrated that Ag-TiO_2 composite extends the photocatalytic activity to visible

light and enhances the antimicrobial properties for *Gram* positive and *Gram* negative bacteria [15].

TiO_2 and Ag-TiO_2 NPs can be obtained through several methods, including sol-gel [16], co-precipitation, hydrothermal, impregnation, electrochemical, microwave discharge methods [17], etc. The electrochemical route represents one of the simplest and cost-effective procedures to synthesize these NPs. Kim and Mohanty [18] reported the electrochemical synthesis of TiO_2 nanotubes, nanograss, and nanolace using aqueous electrolytes. A promising alternative to aqueous electrolytes during electrochemical synthesis is represented by deep eutectic solvents (DESs) [19], a class of ionic liquids, that are environmentally friendly, cost-effective, and stable with respect to air and moisture [17, 18]. Electrochemical synthesis in DESs ensures growth and nucleation control of NPs, which leads to well defined nanostructures [22].

In our previous work [23], Ag-TiO_2 composites electrochemically synthesized in DES showed enhanced photocatalytic performance over pure TiO_2 for MO dye degradation. The electrochemical synthesis was performed using the pulsed reverse current (PRC) method. The duration and the current density of the T_{on} and T_{off} times have been optimized to ±100 mA, 100 ms and 200 ms, respectively. The overall duration of the electrochemical process was varied from 1 h to 3 h and 6 h, respectively, being labelled as Ag-TiO_2-1h, Ag-TiO_2-3h and Ag-TiO_2-6h. The composites synthesized for 1 h, 3 h, and 6 h presented distinct behaviours. Ag-TiO_2-3h presented surface plasmon resonance (SPR) effect, which led to better absorption of the light and better photodegradation properties. The other composite synthesized for 6 h, presented lower photodegradation performance compared to the material synthesized for 3 h due to the formation of silver oxides attributed to the longer deposition time. However, intermediate electrochemical synthesis times have not yet been explored.

Therefore, the aim of this study is to investigate the Ag-TiO_2 composite synthesized electrochemically in DES by PRC deposition at an intermediate deposition time of 5 h. The comparison between the 5h composite and the samples investigated before, Ag-TiO_2-3h and Ag-TiO_2-6h, will shed light on the optimal deposition window for the electrochemical synthesis of Ag-TiO_2 composites in DESs.

2. Materials and methods

2.1 Chemicals

Choline chloride (ChCl) and ethylene glycol (EG) were purchased from Thermo Scientific. Poly (N-vinyl pyrrolidone) (PVP 10) and tetrabutylammonium bromide (TBAB) were purchased from Sigma Aldrich. Ethanol (EtOH) was from

Ingen Laboratory, Timisoara, Romania, while methyl orange (MO) was provided by Polymed Trade, Bucharest, Romania. All chemicals were used as received.

2.2. DES preparation

To obtain the DES electrolyte, ChCl was mixed with EG in a 1:2 molar ratio under continuous stirring at 70 °C until a transparent liquid was formed. The mixture remained liquid after cooling down to room temperature.

2.3 Electrochemical synthesis of TiO_2 NPs and Ag-TiO_2 composite

TiO_2 NPs employed in the composite synthesis were obtained using the sacrificial anode method previously reported [20]. Ag-TiO_2-5h composite was synthesized using a pulsed reverse current (PRC) method, schematically presented in Fig. 2.

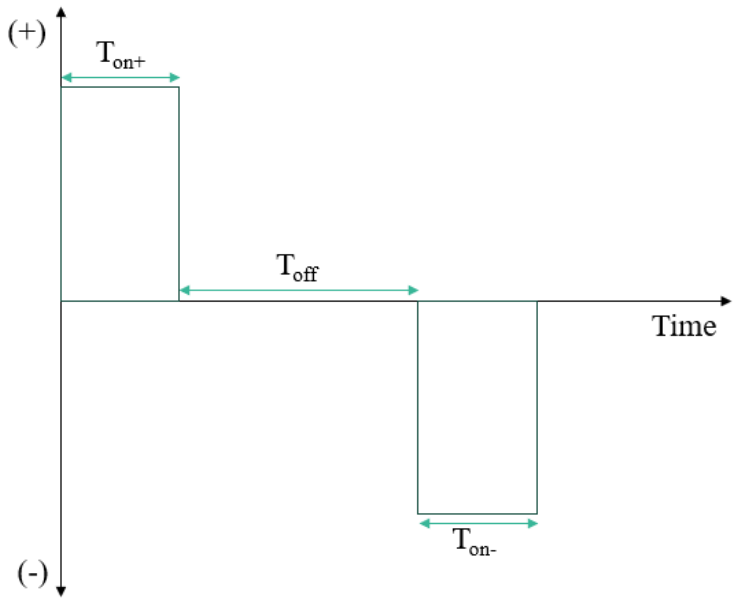

Fig. 2. The pulse plating wave of the electrochemical synthesis of Ag-TiO_2-5h composite.

The electrochemical conditions are described in detail in our previous work, the only difference being the total deposition time of 5 h [23]. Briefly, the anodic (T_{on}^{+}) and cathodic (T_{on}^{-}) currents were fixed at 100 mA, and the duration of the pulse was set to 100 ms. Between these pulses, a period during which no current is applied, namely T_{off}, was fixed for 200 ms. The overall duration of the electrochemical process is 5 h. After the synthesis process, the resulting gel was

cleaned with ethanol and water, dried at 100 °C, and calcined at 600 °C for 2 h and 30 min.

2.4 Characterization Techniques

Field Emission Scanning Electron Microscopy (FESEM, Nova NanoSEM 630 equipment) operated at 10 kV was used to examine the morphology of the samples. For the composition, an Energy Dispersive X-Ray analysis (EDS) was performed using Smart Insight AMETEK.

To get insights into the crystallinity of the material and the phases present, a 9 kW X-ray Diffractometer (XRD) from Rigaku SmartLab (CuKα1 source - λ = 0.15406 nm) was used. The 2θ range varied from 10° to 70°. The measurements were done at room temperature.

The surface charge of TiO_2 at different pH values was assessed using electrophoretic light scattering (ELS) with a Beckman Coulter (USA) DelsaTMNano C instrument. A laser diode of 658 nm illuminated the nanoparticles, producing time-dependent fluctuations in the intensity of laser light, while the angle for Zeta potential measurements was 15°. The measurements were performed at 25ºC and the DelsaNano 3.73/2.30 software was used to further process the data.

Brunauer-Emmett-Teller (BET) nitrogen adsorption analyser from TriStar Plus-Micromeritics, Norcross was employed to determine the specific surface area and pore volume of the samples.

2.5. Photodegradation procedure

The photoreactivity of the TiO_2 NPs and Ag-TiO_2-5h composite was evaluated under UV radiation for the degradation of MO dye (10 mg/mL, pH = 3). 1 g/L of nanopowder was added into 25 mL dye solution, and it was magnetically stirred in the dark for 30 min to establish the adsorption equilibrium. After that, it was irradiated with a UV lamp (λ = 365 nm, 6 W, Wiesloch) under continuous stirring. The residual dye concentration was quantified every 60 min of UV irradiation for a total exposure time of 360 min. The chromophore absorption maxima at 504 nm were used to assess the degradation efficiency. All experiments took place in a black box to prevent the dye from being exposed to external light. The schematic setup diagram is presented in Fig. 3.

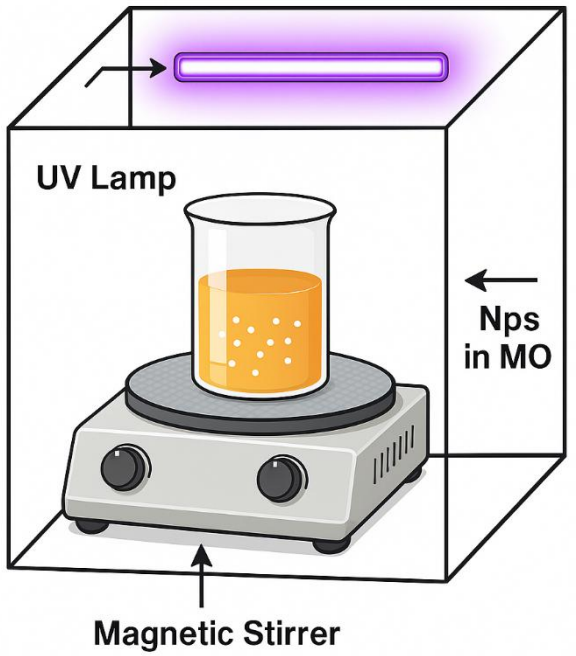

Fig. 3. The schematic diagram of the photodegradation procedure.

3. Results and discussions

In Fig. 4, SEM images of as-synthesized, amorphous TiO_2 powder are presented at 100,000× and 200,000×. The NPs are agglomerated and present spherical shapes. This morphology and the low defined nanoparticles boundaries indicate an amorphous phase, which was also confirmed by the XRD pattern, where a broad peak at 28˚ is noticed. (Fig. 5).

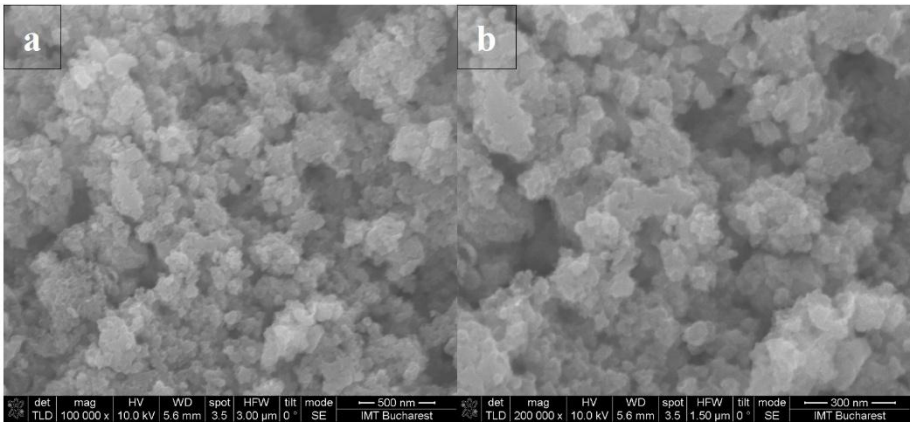

Fig. 4. SEM micrographs of amorphous TiO_2 at: a) 100,000× and b) 200,000×.

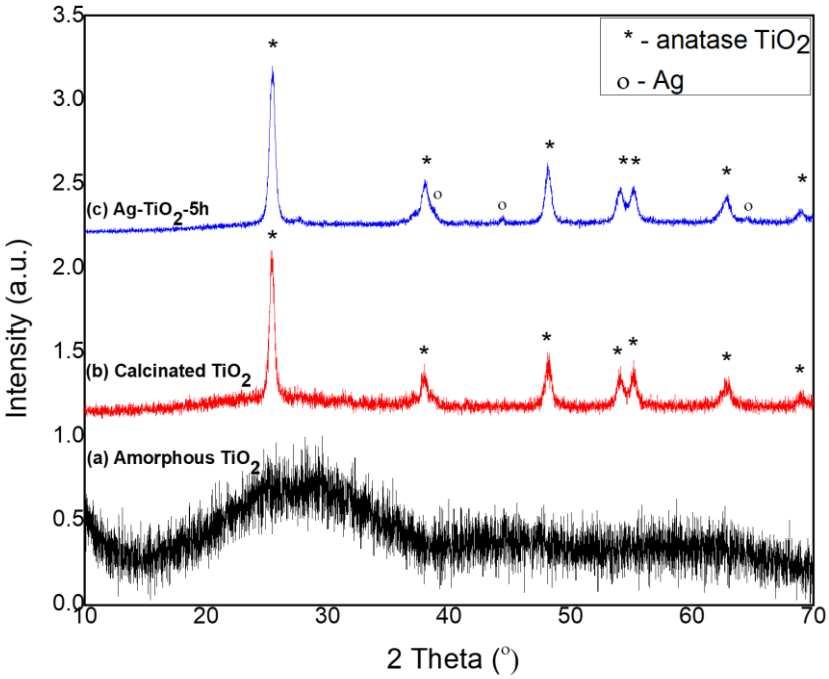

Fig. 5. XRD diffractograms of:
(a) amorphous TiO_2, (b) calcined TiO_2 and (c) Ag-TiO_2-5h.

After calcinating at 600˚C for 2 h and 30 min, the amorphous as-synthesized TiO_2 powder transforms into crystalline, as reflected by the narrow and intense diffraction peaks located at 2θ = 25.4˚, 37.1˚, 48.0˚, 53.9˚, 55.4˚, 62.9˚ and 68.9˚ characteristic of the anatase phase (a - TiO_2 card no. 21-1272).

The analysis of the mean crystallite size by using Scherrer equation led to a value of ~ 14 nm, indicating the polycrystalline nature of the material after the calcination. In addition, for Ag-TiO_2 sample, small diffraction peaks at 2θ = 38.0˚, 44.4˚ and 64.5˚ (Ag card no. 01-1164) can be noticed, these coming from cubic Ag.

The SEM images, presented in Fig. 6, show nanoparticles with spherical morphology, like amorphous TiO_2, but due to the calcination process, diameter ranges between 4 and 18 nm with a mean diameter (*MD*) of 11.99 and a standard deviation (*SD*) of 2.55, as shown in Fig. 7.

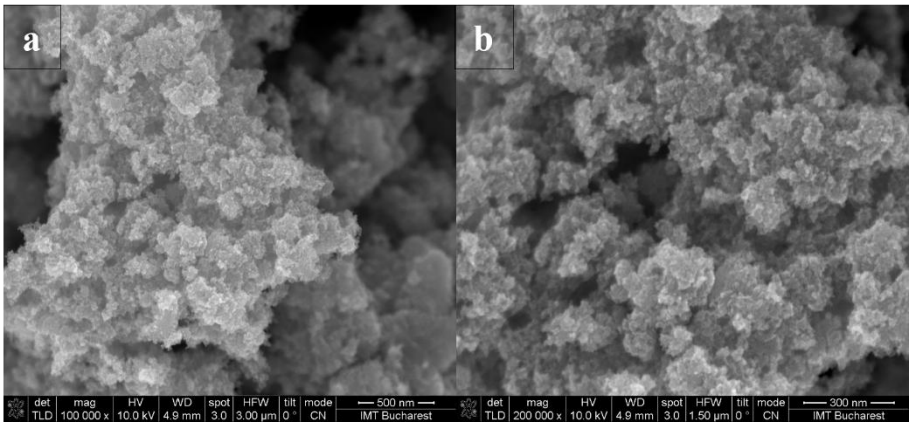

Fig. 6. SEM micrographs of anatase TiO_2 at: a) 100,000× and e) 200,000×.

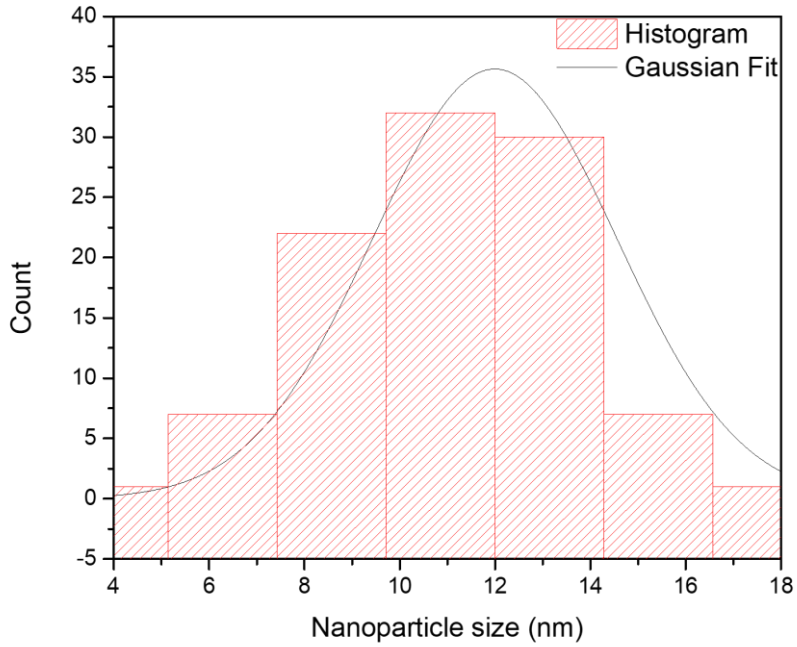

Fig. 7. Particle size distribution of calcined TiO_2 and the Gaussian fit of the distribution.

To further investigate the surface properties and the potential interaction of TiO_2 NPs with the MO dye, the Zeta potential of calcinated TiO_2 was measured at different values of pH (Fig. 8). In acidic conditions (pH 3), the Zeta potential of TiO_2 NPs has positive values (+33.83 mV), which shows a strong electrostatic affinity for anionic azo dyes such as MO. At the pH 5-6, the Zeta potential decreases significantly, approaching zero. The Point of Zero Charge for the TiO_2 was

identified at approximately pH 5.8. Beyond this point, the surface becomes negatively charged (at neutral or alkaline pH). Similar results were obtained by Liao et al. [24] in the same calcination conditions of TiO_2 NPs.

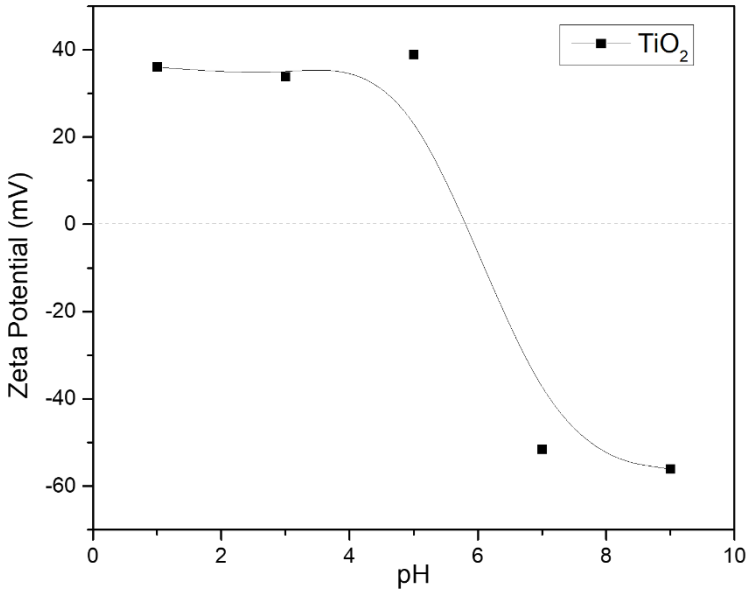

Fig. 8. Variation of Zeta Potential with pH for the calcinated TiO_2.

SEM images of Ag-TiO_2-5h composite electrochemically synthesized at 100,000× and 200,000× are presented in Fig. 9.

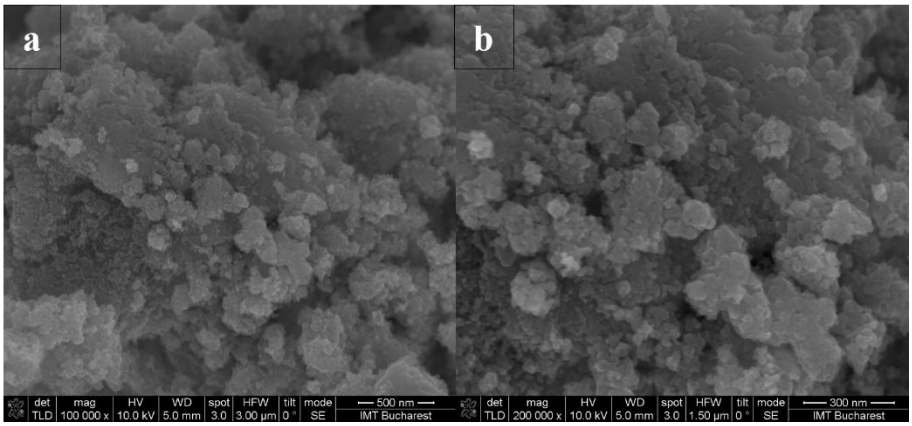

Fig. 9. SEM micrographs of Ag-TiO_2-5h composite at:
a) 100,000× and b) 200,000×.

According to these images, it was found that the obtained Ag-TiO_2-5h composite presents grains with spherical morphology, whose size ranges between 10 and 40 nm (MD = 22.62, SD = 5.92), which is confirmed by the particle size distribution analysis, described by a Gaussian fit (Fig. 10). Compared to the anatase TiO_2, Ag-TiO_2-5h composite presents more agglomerated and larger NPs due to the Ag decoration.

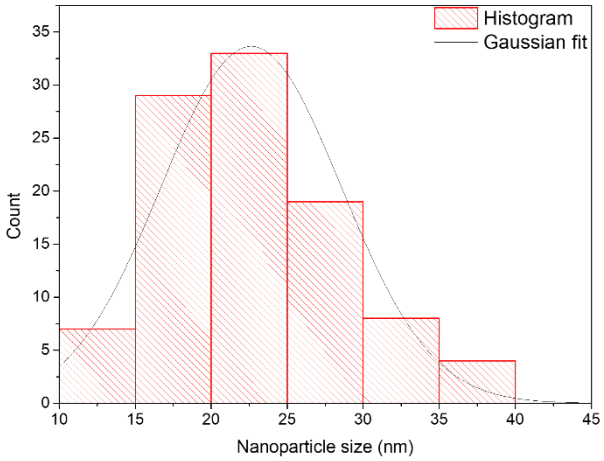

Fig. 10. Particle size distribution of Ag-TiO_2-5h composite and the Gaussian fit of the distribution.

To further verify the presence of Ag in the sample, a complementary analysis was performed using EDS (Fig. 11).

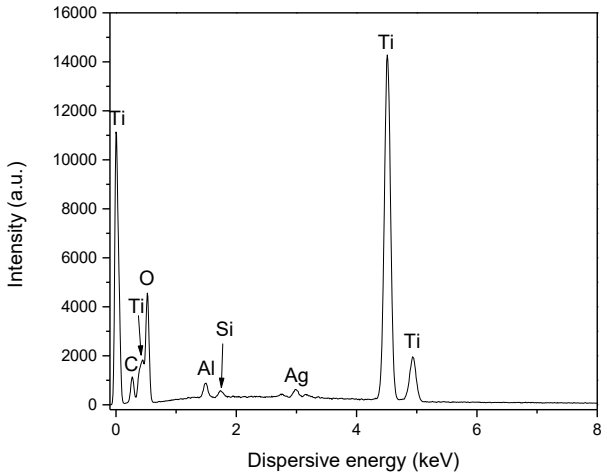

Fig. 11. EDS spectrum of Ag-TiO_2-5h composite.

Peaks associated with titanium (Ti) and oxygen (O) are shown in the EDS spectrum alongside the peak for silver (Ag) at 3 keV, which confirms the presence of Ag on the TiO_2 surface. Other peaks of aluminium (Al), silicon (Si) and carbon (C) shown in the EDS spectrum are due to the sample holder and the carbon coating (Fig. 11). No contaminants were detected in the sample, which indicates that a clean electrochemical synthesis in DESs was performed.

For the Ag-TiO_2 composite synthesized for 5h, XRD analysis confirmed the presence of metallic Ag (see Fig. 5), without peaks associated with silver oxides, which were in the previous work, for synthesis times of 6 h [23]. As confirmed by the XRD analysis presented in Fig. 5, the Ag-TiO_2 composite synthesized for 5 h contains metallic Ag without peaks associated with silver oxide, as observed for the synthesis time of 6h [23].

From the BET analysis, Ag-TiO_2-5h composite presents a specific surface area of 19.03 $m^2\ g^{-1}$, a pore width of 9.4 nm and a total pore volume of 0.047 cm^3. Compared to anatase TiO_2 NPs, which present a specific surface area of 23.05 $m^2\ g^{-1}$, a slight decrease is noticed for the Ag-TiO_2-5h composite. The decrease can be attributed to the partial blocking of TiO_2 pores with Ag NPs. Despite that, the Ag-TiO_2-5h composite presents a slightly increased surface area than the Ag-TiO_2-6h composite (17.75 $m^2\ g^{-1}$), which may make this composite an alternative for the Ag-TiO_2-3h composite in photodegradation.

The degradation of MO under UV light was investigated using TiO_2 NPs and Ag-TiO_2-5h composite. The absorbance of MO decreases proportionally with the irradiation time for both samples. After 6 h of exposure of MO to UV in the presence of TiO_2 NPs and Ag-TiO_2-5h composite, it was demonstrated that Ag-TiO_2-5h composite presents better photocatalytic activity than TiO_2 NPs, as it can be seen in Figs. 12 and 13. The colour removal efficiency after 360 min of exposure was 66.78 % for TiO_2 NPs and 74.18 % for Ag-TiO_2-5h composite (Fig. 12b). This confirms that decorating TiO_2 NPs with metallic Ag NPs improves the photodegradation efficiency even at 5 h of electrochemical synthesis because it promotes effective charge separation and reduces electron-hole recombination. This mechanism enhances the generation of ROS (•OH and •O2), which are responsible for MO dye degradation. Similar behavior was reported for Ag modified TiO_2 systems by Merdoud et al. [25].

The pseudo-first-order reaction rate constant (k_{app}) of the photodegradation process was calculated using the slope of the fit of $\ln(C/C_0)$ vs time (Eq. (1)) under UV irradiation (Fig. 14). Ag-TiO_2-5h presents a decay rate of 3.89×10^{-3} min^{-1} for degradation under UV light, which is lower than the decay rate of Ag-TiO_2-3h and Ag-TiO_2-6h, but higher than the decay rate of TiO_2 NPs and Ag-TiO_2-1h composite, previously calculated [23].

$$-ln\frac{C}{C_0} = k_{app}t \quad (1)$$

where C is the MO concentration at different irradiation times (t) and C_0 is the initial concentration of MO.

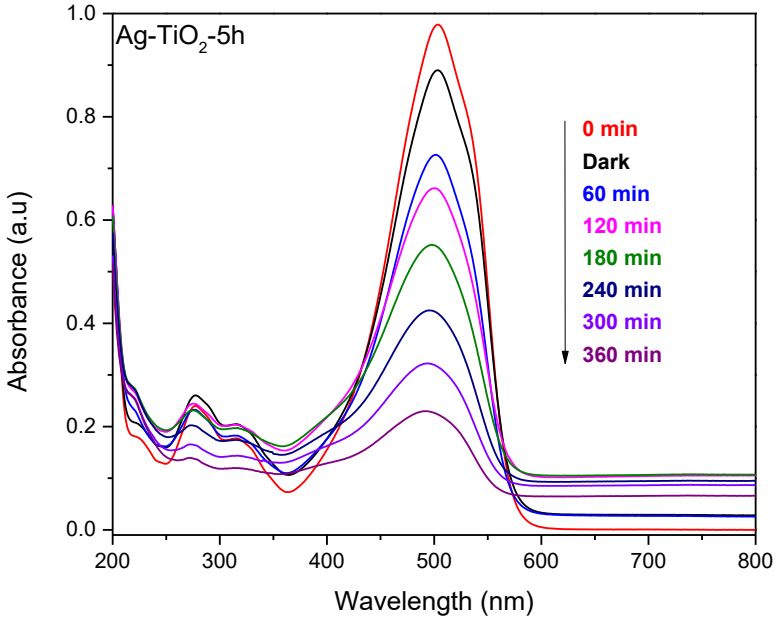

Fig. 12. Absorption spectra to highlight the photocatalytic degradation of a methyl orange solution in the presence of Ag-TiO_2-5h composite.

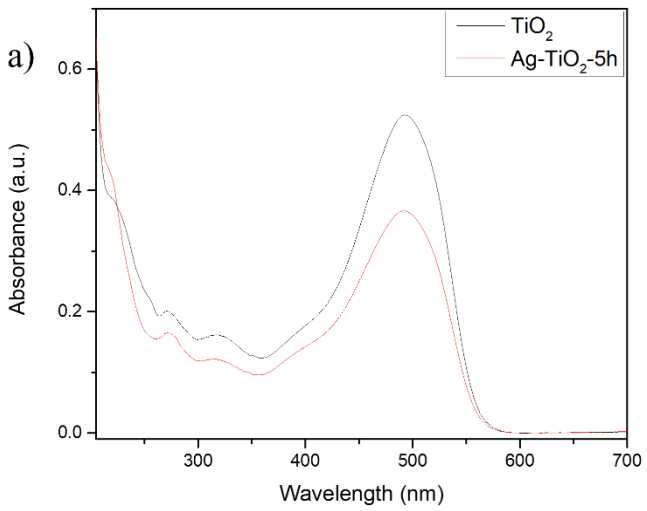

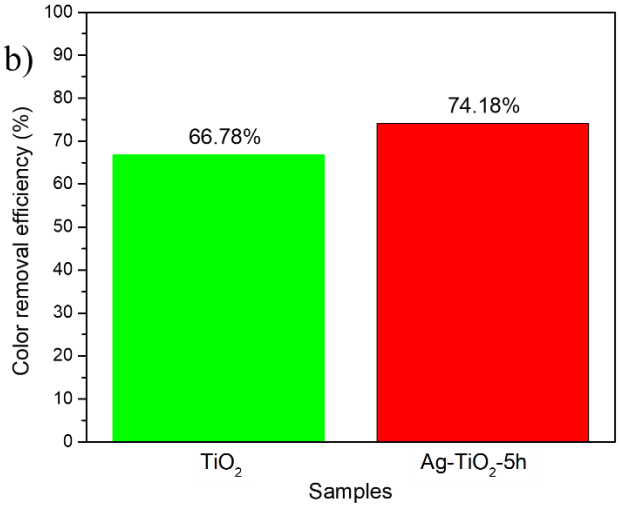

Fig. 13. a) Comparison of the photodegradation efficiency after 360 min of UV irradiation for TiO_2 NPs and Ag-TiO_2-5h composite and b) Bar diagram of colour removal efficiency (%) of MO for TiO_2 and Ag-TiO_2-5h composite.

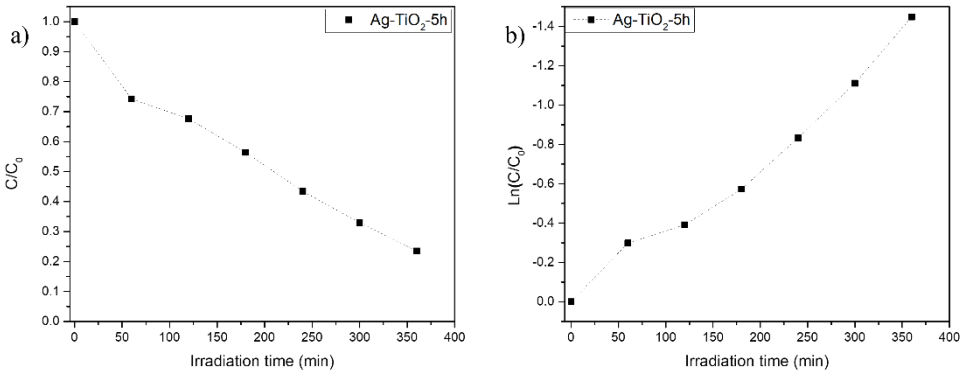

Fig. 14. a) MO dye after various UV irradiation times in the presence of Ag-TiO_2-5h composite and b) ln(C/C_0) versus UV irradiation time graph.

6. Conclusion

In this work, an Ag-TiO_2-5h composite was successfully synthesized by an innovative and eco-friendly electrodeposition method using a green electrolyte,

namely a deep eutectic solvent based on choline chloride. This approach is sustainable and presents low toxicity and high-performance results.

Scanning Electron Microscopy results showed spherical morphology for amorphous TiO_2, crystalline TiO_2 and Ag-TiO_2-5h composite. The average particle size diameter was found to be approximately 12 nm for crystalline TiO_2, respectively 22 nm for Ag-TiO_2-5h composite due to the decoration with silver. X-Ray Diffraction pattern confirmed the presence of metallic silver, without the silver oxides noticed for the sample at 6 hours of synthesis. Brunauer-Emmett-Teller calculations showed that the composite has a mesoporous structure, with a specific surface area of 19.03 $m^2\ g^{-1}$. Furthermore, Zeta potential analysis of the TiO_2 showed a high positive charge of +33.83 mV at pH 3, which demonstrates a strong electrostatic affinity for the anionic azo dyes such as methyl orange.

Photocatalytic tests for the degradation of methyl orange dye were validated. The Ag-TiO_2-5h catalyst demonstrated achieved a colour removal efficiency of 74.18%, outperforming pure TiO_2, which achieved a 66.78% efficiency, after 360 minutes of exposure to UV light. Accordingly, the interval between 3 and 5 h represents the optimal window for synthesizing photocatalytically active Ag-TiO_2 composites.

The study confirms that the Ag-TiO_2-5h composite maintains photocatalytic properties while avoiding the drawbacks which appear at longer deposition times like 6 h of synthesis. Future work may focus on reusability and photodegradation performance of this composite under visible-light irradiation and in real wastewater samples, as well as on antimicrobial studies for water treatment to expand its potential applications.

Acknowledgment

The present work was supported by the Romanian National Grant GNAC ARUT 2023 project (No. 7/06.10.2023), NANO_NP_DES, entitled "Electrochemical synthesis of hybrid nanoparticles Ag/TiO_2 and Ag/ Fe_3O_4 with biomedical applications".

Also, the work was supported by the IMT Core Program μNanoEl, within the PNCDI IV 2022-2026, carried out with the support of Romanian Ministry of Education and Research, project 2307 contract no 8N/03.01.2023. National and European funds financially supported the work through FCT under Research Grant UIDB/00081/2025 (https://doi.org/10.54499/UID/PRR/00081/2025)- CIQUP, LA/P/0056/2020 (https://doi.org/10.54499/LA/P/0056/2020) – IMS. Portuguese Recovery and Resilience Plan and by the NextGeneration EU European funds in its component 12 – Sustainable Bioeconomy, Investment under project Bioshoes4All (TC-C12-i01).

REFERENCES

[1] P.C. Dey and R. Das, "Spectrochimica Acta Part A : Molecular and Biomolecular Spectroscopy Enhanced photocatalytic degradation of methyl orange dye on interaction with synthesized ligand free CdS nanocrystals under visible light illumination," Spectrochim. Acta Part A Mol. Biomol. Spectrosc., vol. 231, p. 118122, 2020, doi: 10.1016/j.saa.2020.118122.

[2] M. F. Hanafi and N. Sapawe, "Materials Today : Proceedings Influence of pH on the photocatalytic degradation of methyl orange using nickel catalyst," Mater. Today Proc., vol. 31, pp. 339–341, 2020, doi: 10.1016/j.matpr.2020.06.094.

[3] S. Stojadinovi, "Photocatalytic Degradation of Methyl Orange in Wastewater Using TiO_2 - Based Coatings Prepared by Plasma Electrolytic Oxidation of Titanium : A Review," 2025.

[4] C. Series, "Degradation performance of methyl orange by TiO_2 photocatalyst from green synthesis Degradation performance of methyl orange by TiO_2 photocatalyst from green synthesis," 2024, doi: 10.1088/1742-6596/2900/1/012001.

[5] W. Deligeer, Y. W. Gao, and S. Asuha, "Applied Surface Science Adsorption of methyl orange on mesoporous ∥ -Fe_2O_3 / SiO_2 nanocomposites," Appl. Surf. Sci., vol. 257, no. 8, pp. 3524–3528, 2011, doi: 10.1016/j.apsusc.2010.11.067.

[6] V. Etacheri, C. Valentin, and J. Schneider, "ARROW @ TU Dublin Visible-Light Activation of TiO_2 Photocatalysts : Advances in Theory and Experiments," 2015, doi: 10.1016/j.jphotochemrev.2015.08.003.

[7] C. Langa and N. C. Hintsho-mbita, "Plant and bacteria mediated synthesis of TiO 2 NPs for dye degradation in water . A review," Chem. Phys. Impact, vol. 7, no. July, p. 100293, 2023, doi: 10.1016/j.chphi.2023.100293.

[8] J. Dai, Y. Wu, and Y. Yao, "ZnO / TiO_2 photocatalysts for degradation of methyl orange by low-power irradiation," vol. 108, no. 30, pp. 1–25, 2025, doi: 10.1177/00368504251322606.

[9] P. Tzevelekidis et al., "Visible-light-activated antibacterial and antipollutant properties of biocompatible Cu-doped and Ag-decorated TiO_2 nanoparticles," Heliyon, vol. 10, no. 17, p. e35634, 2024, doi: 10.1016/j.heliyon.2024.e35634.

[10] E. A. apsusc. 2019. 01. 077. pdf. M. Mihai et al., "Self-Sustained Three-Dimensional Macroporous TiO2-Graphene Photocatalyst for Sunlight Decolorization of Methyl Orange," Nanomaterials, vol. 12, no. 24, 2022, doi: 10.3390/nano12244393.

[11] A. Zanfir, G. Voicu, B. Alina-ioana, D. Gogan, and O. Oprea, "Synthesis and characterization of titania-silica fume composites and their influence on the strength of self-cleaning mortar," vol. 140, no. December 2017, pp. 157–163, 2018, doi: 10.1016/j.compositesb.2017.12.032.

[12] W. Baran and M. Cholewi, "A New Mechanism of the Selective Photodegradation of Antibiotics in the Catalytic System Containing TiO 2 and the Inorganic Cations," 2021.

[13] S. Kader, R. Al-mamun, and B. Kabir, "Environmental Technology & Innovation Enhanced photodegradation of methyl orange dye under UV irradiation using MoO 3 and Ag doped TiO_2 photocatalysts," Environ. Technol. Innov., vol. 27, p. 102476, 2022, doi: 10.1016/j.eti.2022.102476.

[14] L. Anicai, A. Petica, D. Patroi, V. Marinescu, P. Prioteasa, and S. Costovici, "Electrochemical synthesis of nanosized TiO2 nanopowder involving choline chloride based ionic liquids," Mater. Sci. Eng. B, vol. 199, pp. 87–95, 2015, doi: 10.1016/j.mseb.2015.05.005.

[15] H. Chakhtouna, H. Benzeid, N. Zari, A. el kacem Qaiss, and R. Bouhfid, "Recent progress on Ag/TiO_2 photocatalysts: photocatalytic and bactericidal behaviors," Environ. Sci. Pollut. Res., vol. 28, no. 33, pp. 44638–44666, 2021, doi: 10.1007/s11356-021-14996-y.

[16] K. Balachandran, G. Vijayakumar, S. Mageswari, A. Preethi, and M. S. V. Senan, "Synthesis and Characterization of Ag-Decorated TiO 2 Nanoparticles for Photocatalytic Application," vol. 10, no. 4, pp. 13–18, 2021.

[17] M. Mogildea et al., “Synthesis of the Titanium Oxides Using a New Microwave Discharge Method,” vol. 26, no. 5, p. 2173, 2025.

[18] Y. Kim and S. K. Mohanty, “Electrochemical Synthesis and Morphological Analysis of Titanium Dioxide Nanostructures : Nanotubes , Nanograss , and Nanolace,” 2025, doi: 10.1002/adem.202402227.

[19] H. Xia, M. Ren, Y. Zou, and S. Qin, “and Mechanical Properties : The Role of Water,” Green Chem. Eng., vol. 2, no. 4, pp. 359–367, 2020, [Online]. Available: https://doi.org/10.1016/j.gce.2021.06.001

[20] A. Petica, A. Florea, C. Gaidau, D. Balan, and L. Anicai, “Synthesis and characterization of silver-titania nanocomposites prepared by electrochemical method with enhanced photocatalytic characteristics, antifungal and antimicrobial activity,” J. Mater. Res. Technol., vol. 8, no. 1, pp. 41–53, 2019, doi: 10.1016/j.jmrt.2017.09.009.

[21] A. Cojocaru et al., “Electrochemical preparation of Ag nanoparticles involving choline chloride-glycerol deep eutectic solvents,” Bulg. Chem. Commun., vol. 49, no. June, pp. 194–204, 2017.

[22] E. L. Smith, A. P. Abbott, and K. S. Ryder, “Deep Eutectic Solvents (DESs) and Their Applications,” Chem. Rev., vol. 114, no. 21, pp. 11060–11082, 2014, doi: 10.1021/cr300162p.

[23] I. Petcu et al., “Applied Surface Science Advances Pulsed reverse electrochemical synthesis of Ag-TiO_2 composites from deep eutectic solvents : Photocatalytic and antibacterial behaviour,” vol. 27, no. April, 2025, doi: 10.1016/j.apsadv.2025.100749.

[24] D. L. Liao, G. S. Wu, and B. Q. Liao, “Colloids and Surfaces A : Physicochemical and Engineering Aspects Zeta potential of shape-controlled TiO_2 nanoparticles with surfactants,” vol. 348, pp. 270–275, 2009, doi: 10.1016/j.colsurfa.2009.07.036.

[25] R. Merdoud et al., “Methyl Orange Degradation Using Ag-Doped TiO_2, H_2O_2, and Hydrodynamic Cavitation,” 2025, doi: 10.1021/acsomega.5c00034.